# DESTRIPING HYPERSPECTRAL IMAGERY BY ADAPTIVE ANISOTROPIC TOTAL VARIATION AND TRUNCATED NUCLEAR NORM

*Ting Hu*[1], *Na Liu*[2], *Wei Li*[1], *Ran Tao*[1*], *Feng Zhang*[1], *and Paul Scheunders*[3]

[1] School of Information & Electronics, Beijing Institute of Technology, China
[2] College of Information Science & Technology, Beijing University of Chemical Technology
[3] IMEC-Vision Lab, Department of Physics, University of Antwerp, Belgium

## ABSTRACT

Destriping is an important hyperspectral image processing procedure. Many variation-based methods show adequate destriping performance. However, global variation constraints cause loss of texture information in unstriped image regions. To alleviate this effect, we propose an adaptive anisotropy total variation method to adaptively smoothen the striped regions. Furthermore, considering the highly linear relationship among stripes, we introduce, for the first time, the truncated nuclear norm to constrain the rank of the stripes to 1. When combining the adaptive anisotropy total variation and the truncated nuclear norm, a hyperspectral image destriping model is established, which can easily be solved by the alternating direction method of multipliers (ADMM). Experiments demonstrate the effectiveness and superiority of the proposed destriping method.

***Index Terms***— Hyperspectral image, destriping, adaptive anisotropy total variation, truncated nuclear norm

## 1. INTRODUCTION

Hyperspectral images acquired by pushbroom sensors often suffer from along-track (vertical) stripes, which greatly reduce their applicability for visual interpretation and automated analysis. Nowadays, a plethora of works on hyperspectral destriping has been investigated. Destriping algorithms can be classified as either statistical [1], filtering-based [2] or optimization-based methods [3–6]. Because they make strict statistical assumptions on stripes, statistical methods are of limited practicability [7]. Filtering-based destriping methods often show blurring and staircase effects. [8].

Recently, optimization-based methods that incorporate proper prior constraints into the ill-posed inverse destriping problem, have attracted much attention because of their superior performance. By merging the Huber-Markov variation prior into a maximum a posteriori framework, a representative destriping and impainting method [3] was proposed. Later, Chang *et al*. [4] achieved better destriping by minimizing a spectral-spatial anisotropy total variation of the clean image. An outstanding destriping approach was proposed [6], co-regularizing the latent image and stripes, where the image and stripes were constrained by the anisotropy total variation and the nuclear norm, respectively. However, these variation-based methods minimize the global variation of the latent image, resulting in texture information loss in the unstriped image parts. In [5], an optimized model, combining the low-rank regularization of images and the control of the upper cardinality bound of noise, produced adequate destriping results. However, these destriping algorithms require manual tuning of parameters when regularizing stripes.

To overcome the above drawbacks, a new hyperspectral image destriping method is proposed. Specifically, in order to preserve the texture information in the unstriped regions, while ensuring smoothness in the striped regions, an adaptive anisotropic total variation method is proposed. Since theoretically, each stripe can be expressed as a linear combination of all other stripes, stripes have rank 1. As the truncated nuclear norm can better control the rank of a matrix [9], we propose to apply the truncated nuclear norm to constrain stripes, such that no manual tuning parameter is required. Finally, a destriping model, co-regularizing the adaptive anisotropic total variation and the truncated nuclear norm (AATT) is established, and can be easily solved with the alternating direction method of multipliers (ADMM).

The reminder of the paper is arranged as follows. In Sec. 2, the proposed destriping model is explained. Experimental results and discussion are presented in Sec. 3, while a summary is given in Sec. 4.

## 2. PROPOSED DESTRIPING MODEL

A striped image can be expressed as:

$$\mathbf{Y} = \mathbf{I} + \mathbf{S}, \tag{1}$$

where $\mathbf{Y}$, $\mathbf{I}$, $\mathbf{S} \in \mathbb{R}^{M\times N\times B}$ represent the striped image, the clean image, and stripes, respectively, and $M$, $N$, and $B$ denote the number of rows, columns and bands of the image in

This work was supposed in part by the National Natural Science Foundation of China under Grants Nos. 61922013, 61421001 and U1833203.
(Email: rantao@bit.edu.cn)

turn. In this paper, a new model is proposed for destriping by estimating $\mathbf{I}$ and $\mathbf{S}$ from $\mathbf{Y}$.

First, an adaptive anisotropy total variation method is proposed to adaptively perform smoothness regularization, limited to the striped regions, so that texture information is preserved in the unstriped regions. Its key design idea is that the regularization parameters are controlled by the gradients of the stripes, such that no variation constraint is posed on regions without stripe gradients. Since vertical stripes have no vertical gradient, the proposed adaptive variation regularization is only applied in the spectral and horizontal directions:

$$||\mathbf{I}||_{AATV} = ||\mathbf{\Lambda}_1 \cdot \bigtriangledown_x \mathbf{I}||_1 + ||\mathbf{\Lambda}_2 \cdot \bigtriangledown_z \mathbf{I}||_1, \tag{2}$$

where $||\mathbf{I}||_{AATV}$ expresses the adaptive anisotropy total variation of the clean image, $\mathbf{\Lambda}_1 = \min(|\bigtriangledown_{\mathrm{x}} \mathbf{S}|, \beta_{\mathrm{x}})$ and $\mathbf{\Lambda}_2 = \min(|\bigtriangledown_{\mathrm{z}} \mathbf{S}|, \beta_{\mathrm{z}})$ are the regularization parameter tensors, dependent on the spatial horizontal and spectral gradients of stripes, respectively, for an adaptive variation minimization, "$\cdot$" is the element-by-element multiplication operation, $\bigtriangledown_x$ denotes the horizontal gradient operator, identical to the convolution with mask $[1, -1]$. Similarly, $\bigtriangledown_z$ represents the along-spectrum gradient operator. The minimum threshold function $\min(\cdot)$ avoids possible oversmoothing, caused by overly large regularization parameters, with $\beta_x$ and $\beta_z$ being the thresholds along the horizontal and spectral directions, respectively.

Theoretically, stripes are linearly dependent on each other, meaning that they have rank 1. Since the truncated nuclear norm is able to accurately constrain the rank of a matrix [9], the truncated nuclear norm is utilized to constrain the rank of stripes to 1. This rank constraint for stripes avoids the manual tuning of a parameter.

Combining the above variation and rank regularization, the proposed destriping model is obtained:

$$\min_{\mathbf{I},\mathbf{S}} \Big\{ \frac{1}{2}||\mathbf{Y} - \mathbf{I} - \mathbf{S}||_F^2 + ||\mathbf{I}||_{AATV} + \sum_{b=1}^{B} ||\mathbf{S}_b||_r \Big\}, \tag{3}$$

where the first term is the data fidelity term, the other two are the regularization terms. $||\mathbf{S}_b||_r = \sum_{n=r}^{L} \sigma_n(\mathbf{S}_b)$ is the truncated nuclear norm of $\mathbf{S}_b$, $\mathbf{S}_b$ is band $b$ of the stripes image, $L$ is the number of nonzero singular values of $\mathbf{S}_b$, and $r$ is set to 2, to constrain the rank of $\mathbf{S}_b$ to 1.

Despite no analytical solution exists for (3), the proposed AATT can be alternately solved under the ADMM framework, as shown in Fig. 1. After introducing auxiliary variables, Lagrangian multipliers and quadratic penalty terms, the

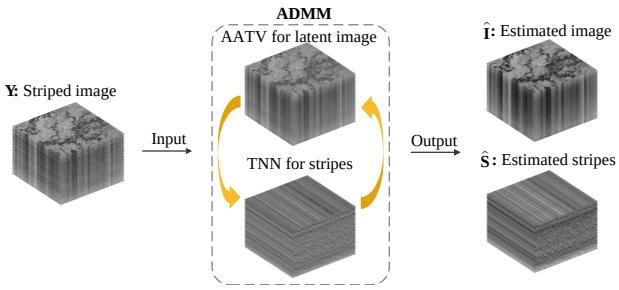


**Fig. 1**. Flowchart of the proposed AATT for hyperspectral destriping. AATV and TNN correspond to the adaptive anisotropy total variation and the truncated nuclear norm, respectively

correspondingly augmented Lagrangian form is obtained:

$$\begin{aligned}\mathcal{L}(\mathbf{Y},\mathbf{I},\mathbf{S},\mathbf{W}_j,\mathbf{A}_j) &= \frac{1}{2}||\mathbf{Y} - \mathbf{I} - \mathbf{S}||_F^2 \\ &+ ||\mathbf{\Lambda}_1 \cdot \mathbf{W}_1||_1 + ||\mathbf{\Lambda}_2 \cdot \mathbf{W}_2||_1 \\ &+ \langle \mathbf{A}_1, \mathbf{W}_1 - \bigtriangledown_x \mathbf{I} \rangle_F + \frac{\alpha}{2}||\mathbf{W}_1 - \bigtriangledown_x \mathbf{I}||_F^2 \\ &+ \langle \mathbf{A}_2, \mathbf{W}_2 - \bigtriangledown_z \mathbf{I} \rangle_F + \frac{\alpha}{2}||\mathbf{W}_2 - \bigtriangledown_z \mathbf{I}||_F^2,\end{aligned} \tag{4}$$

where $\mathbf{W}_j$ are the auxiliary variables, $\mathbf{A}_j$ are the augmented Lagrangian multipliers, and $\alpha > 0$ is the penalty parameter. The solving procedure of the proposed AATT is summarized in Alg. 1, where the superscript $k$ denotes the $k$-th iteration, and $\mathcal{S}(\theta, \phi) = \mathrm{sign}(\theta) \cdot \max(|\theta| - \phi, 0)$ is a soft-threshold function [10].

**Algorithm 1** Destriping by AATT

**Input:** Striped image $\mathbf{Y}$, total number of iterations $K$

1: Initialization $\mathbf{I}^0 = \mathbf{Y}$; $\mathbf{S}^0$, $\mathbf{A}_1^0$, $\mathbf{A}_2^0 = \mathbf{0}$
2: **for** $k = 1 : K$ **do**
3: Update $\mathbf{I}^k$ by solving the following problem in Fourier domain [4]
$\min_{\mathbf{I}} \Big\{ \frac{1}{2} \Big\| \mathbf{Y} - \mathbf{I} - \mathbf{S}^k \Big\|_F^2 + \frac{\alpha}{2} \Big\| \mathbf{W}_1^k - \bigtriangledown_x \mathbf{I} + \frac{\mathbf{A}_1^k}{\alpha} \Big\|_F^2 + \frac{\alpha}{2} \Big\| \mathbf{W}_2^k - \bigtriangledown_z \mathbf{I} + \frac{\mathbf{A}_2^k}{\alpha} \Big\|_F^2 \Big\}$
4: Update $\mathbf{S}^k$ in a band-by-band way, following Theorem 3.1 in [9]
5: Update $\mathbf{W}_1^k$ and $\mathbf{W}_1^k$:
$\mathbf{W}_1^k = \mathcal{S}\big( \bigtriangledown_x \mathbf{I}^{k-1} - \mathbf{A}_1^{k-1}/\alpha, |\mathbf{\Lambda}_1^{k-1}|/\alpha \big)$,
$\mathbf{W}_2^k = \mathcal{S}\big( \bigtriangledown_z \mathbf{I}^{k-1} - \mathbf{A}_2^{k-1}/\alpha, |\mathbf{\Lambda}_2^{k-1}|/\alpha \big)$
6: Update $\mathbf{A}_1^k$ and $\mathbf{A}_1^k$:
$\mathbf{A}_1^k = \mathbf{A}_1^{k-1} + \alpha\big( \mathbf{W}_1^k - \bigtriangledown_x \mathbf{I}^k \big)$,
$\mathbf{A}_2^k = \mathbf{A}_2^{k-1} + \alpha\big( \mathbf{W}_2^k - \bigtriangledown_z \mathbf{I}^k \big)$
7: **end for**
8: return $\mathbf{I}^k$ and $\mathbf{S}^k$ as $\hat{\mathbf{I}}$ and $\hat{\mathbf{S}}$, respectively

**Output:** Estimated image $\hat{\mathbf{I}}$ and estimated stripes $\hat{\mathbf{S}}$

## 3. EXPERIMENTS AND DISCUSSION

Destriping experiments were performed on two synthetically striped images, generated from the Botswana and University of Pavia images [1]. The Botswana image was captured by the NASA EO-1 satellite over the Okavango Delta, Botswana; the University of Pavia image was acquired by the ROSIS sensor over Pavia university. After discarding the water absorption bands, two subimages of size $256 \times 256 \times 145$ and $256 \times 256 \times 93$ are cropped from the Botswana and University of Pavia images, respectively. Both subimages are linearly normalized to $[0, 1]$ before destriping, and restored to the original scale after destriping. The two striped images are artificially produced by adding or subtracting a stripe of intensity $\eta$ to $\mathrm{round}(\gamma \mathrm{N})$ (i.e, a integer obtained by rounding off $\gamma N$, where $\gamma$ denotes the stripe density) columns, randomly selected from each band of the above two subimages.

For a comparative study, we apply the proposed AATT as well as a number of state-of-the-art methods to destripe the synthetic data. The comparison methods are the anisotropic spatial-spectral total variation (ASSTV) [4], low-rank multispectral image decomposition (LRMID) [6], and low-rank matrix recovery (LRMR) [5] methods.

**Table 1**. Metrics on the Botswana image for different levels of stripes.

| Metrics | Method | $\eta = 0.4$ | | | $\eta = 0.6$ | | |
|---|---|---|---|---|---|---|---|
| | | $\gamma$ | | | $\gamma$ | | |
| | | 0.2 | 0.4 | 0.6 | 0.2 | 0.4 | 0.6 |
| PSNR | Striped | 40.20 | 37.19 | 35.40 | 36.68 | 33.67 | 31.87 |
| | ASSTV | 54.16 | 53.16 | 52.11 | 52.13 | 50.97 | 49.97 |
| | LRMID | 55.92 | **54.38** | 53.35 | 53.56 | 52.53 | **51.80** |
| | LRMR | 50.82 | 48.73 | 47.23 | 48.15 | 45.52 | 44.16 |
| | AATT | **56.14** | 54.26 | **53.60** | **54.42** | **52.66** | **51.80** |
| SSIM | Striped | 0.8713 | 0.7723 | 0.6882 | 0.7720 | 0.6177 | 0.5097 |
| | ASSTV | 0.9884 | 0.9872 | 0.9844 | 0.9819 | 0.9793 | 0.9738 |
| | LRMID | 0.9937 | **0.9922** | 0.9881 | 0.9902 | 0.9860 | 0.9841 |
| | LRMR | 0.9832 | 0.9739 | 0.9632 | 0.9700 | 0.9468 | 0.9289 |
| | AATT | **0.9940** | 0.9918 | **0.9901** | **0.9908** | **0.9870** | **0.9848** |
| SAM | Striped | 0.4333 | 0.5791 | 0.6737 | 0.5996 | 0.7665 | 0.8678 |
| | ASSTV | 0.1207 | 0.1382 | 0.1493 | 0.1616 | 0.1772 | 0.2089 |
| | LRMID | 0.1039 | 0.1248 | 0.1363 | 0.1367 | 0.1451 | 0.1531 |
| | LRMR | 0.1476 | 0.1864 | 0.2095 | 0.1906 | 0.2594 | 0.3018 |
| | AATT | **0.0820** | **0.1049** | **0.1069** | **0.1024** | **0.1257** | **0.1449** |
| SID | Striped | 151.79 | 303.84 | 460.69 | 239.26 | 484.27 | 732.82 |
| | ASSTV | 26.89 | 28.79 | 33.79 | 35.03 | 41.36 | 52.42 |
| | LRMID | **20.13** | **22.58** | 32.36 | **25.62** | 35.14 | 39.82 |
| | LRMR | 32.06 | 43.69 | 55.69 | 48.11 | 76.41 | 104.84 |
| | AATT | 22.55 | 26.31 | **29.03** | 27.24 | **33.09** | **38.49** |

As for the parameter settings, $\alpha$ and $K$ are set as $0.1$ and $50$, respectively, while $\mu_x$ and $\mu_z$ are tuned within the ranges $[0.001, 0.03]$ and $[0.001, 0.005]$, respectively. The peak signal-to-noise ratio (PSNR), structural similarity (SSIM), spectral angle mapper (SAM) and spectral information divergence (SID) are calculated to quantitatively assess the destriping effects. Higher values of PSNR and SSIM denote a better reconstruction, while lower values of SAM and SID denote a lower distortion of hyperspectral information.

[1] http://www.ehu.eus/ccwintco/index.php?title=Hyperspectral_Remote_Sensing_Scenes

**Table 2**. Metrics on the University of Pavia image for different levels of stripes.

| Metrics | Method | $\eta = 0.4$ | | | $\eta = 0.6$ | | |
|---|---|---|---|---|---|---|---|
| | | $\gamma$ | | | $\gamma$ | | |
| | | 0.2 | 0.4 | 0.6 | 0.2 | 0.4 | 0.6 |
| PSNR | Striped | 33.29 | 30.28 | 28.49 | 29.76 | 26.75 | 24.96 |
| | ASSTV | 53.31 | 51.85 | 50.73 | 51.17 | 50.13 | 48.83 |
| | LRMID | 54.69 | 53.59 | 52.01 | 52.73 | 51.79 | 49.27 |
| | LRMR | 43.91 | 40.91 | 39.48 | 42.60 | 40.07 | 37.52 |
| | AATT | **55.60** | **54.43** | **53.41** | **54.21** | **53.45** | **51.10** |
| SSIM | Striped | 0.6835 | 0.4760 | 0.3417 | 0.5227 | 0.2863 | 0.1634 |
| | ASSTV | 0.9934 | 0.9904 | 0.9882 | 0.9893 | 0.9854 | 0.9817 |
| | LRMID | 0.9950 | 0.9933 | 0.9908 | 0.9922 | 0.9891 | 0.9827 |
| | LRMR | 0.9543 | 0.9093 | 0.8734 | 0.9388 | 0.8878 | 0.8262 |
| | AATT | **0.9957** | **0.9940** | **0.9928** | **0.9933** | **0.9924** | **0.9886** |
| SAM | Striped | 0.7632 | 0.9300 | 1.0213 | 0.9469 | 1.1001 | 1.1771 |
| | ASSTV | 0.1042 | 0.1135 | 0.1306 | 0.1271 | 0.1493 | 0.1602 |
| | LRMID | 0.0903 | 0.0973 | 0.1156 | 0.1083 | 0.1266 | 0.1584 |
| | LRMR | 0.2634 | 0.3811 | 0.4505 | 0.3046 | 0.4074 | 0.5209 |
| | AATT | **0.0839** | **0.0935** | **0.1014** | **0.1007** | **0.1086** | **0.1279** |
| SID | Striped | 196.87 | 393.03 | 592.06 | 310.83 | 621.43 | 935.79 |
| | ASSTV | 10.13 | 14.19 | 17.42 | 15.85 | 21.23 | 26.19 |
| | LRMID | 7.80 | 10.19 | 13.44 | 11.74 | 15.55 | 24.12 |
| | LRMR | 66.27 | 140.14 | 204.61 | 89.71 | 164.84 | 242.77 |
| | AATT | **6.58** | **8.98** | **10.57** | **10.10** | **11.22** | **16.34** |

The results of the different methods on the images with different levels of stripes are listed in Tables 1 and 2. In addition, for a visual evaluation of the considered algorithms, the destriping results on the images with stripes of intensity $\eta = 0.4$ and density $\gamma = 0.6$ are shown in Figs. 2 and 3. LRMR that poses a low-rank constraint on the clean image obtains the worst destriping performance, probably because stripes are low-rank as well, so that the low-rank constraint prevents a proper destriping. Both AASTV and LRMID perform better. AASTV poses no constraints on the stripes, while LRMID does, but both apply a global TV on the clean image. The best destriping results were obtained by the proposed AATT, due to the adaptive anisotropy TV on the clean image, preserving the unstriped regions, combined with the truncated nuclear norm, for an improved constraining of the stripes.

## 4. CONCLUSION

In order to preserve image information and avoid manual parameters when performing hyperspectral destriping, a method combining an adaptive anisotropy total variation with a truncated nuclear norm was proposed. More specifically, the adaptive anisotropy variation was designed to adaptively

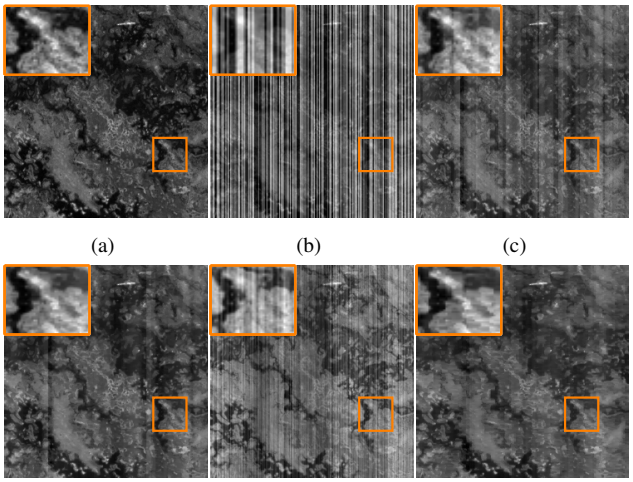

**Fig. 2**. A band selected from the Botswana image. (a) Clean image. (b) Striped image. Destriped images using (c) ASSTV, (d) LRMID, (e) LRMR, and (f) AATT.

smoothen the striped image regions while preserving information in the unstriped regions. To account for the linear relation between stripes, a truncated nuclear norm regularization without any manual parameters was employed to constrain the rank of stripes. The proposed destriping method was effectively optimized under the ADMM framework. Experiments on synthetically striped images confirmed that the proposed approach better removed stripes and preserved information, compared to the state-of-the-art methods.

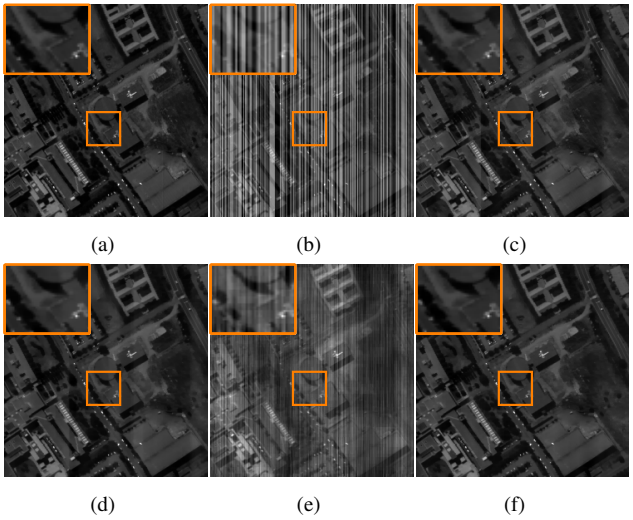

**Fig. 3**. A band selected from the University of Pavia image. (a) Clean image. (b) Striped image. Destriped images using (c) ASSTV, (d) LRMID, (e) LRMR, and (f) AATT.

## 5. REFERENCES


[1] L. Sun, R. Neville, K. Staenz, and H. P. White, "Automatic destriping of hyperion imagery based on spectral moment matching," *Canadian Journal of Remote Sensing*, vol. 34, no. sup1, pp. S68–S81, 2008.

[2] R. Pande-Chhetri and A. Abd-Elrahman, "De-striping hyperspectral imagery using wavelet transform and adaptive frequency domain filtering," *ISPRS Journal of Photogrammetry and Remote Sensing*, vol. 66, no. 5, pp. 620–636, 2011.

[3] H. Shen and L. Zhang, "A MAP-based algorithm for destriping and inpainting of remotely sensed images," *IEEE Transactions on Geoscience and Remote Sensing*, vol. 47, no. 5, pp. 1492–1502, 2009.

[4] Y. Chang, L. Yan, H. Fang, and C. Luo, "Anisotropic spectral-spatial total variation model for multispectral remote sensing image destriping," *IEEE Transactions on Image Processing*, vol. 24, no. 6, pp. 1852–1866, 2015.

[5] H. Zhang, W. He, L. Zhang, H. Shen, and Q. Yuan, "Hyperspectral image restoration using low-rank matrix recovery," *IEEE Transactions on Geoscience and Remote Sensing*, vol. 52, no. 8, pp. 4729–4743, 2014.

[6] Y. Chang, L. Yan, T. Wu, and S. Zhong, "Remote sensing image stripe noise removal: From image decomposition perspective," *IEEE Transactions on Geoscience and Remote Sensing*, vol. 54, no. 12, pp. 7018–7031, 2016.

[7] H. Carfantan and J. Idier, "Statistical linear destriping of satellite-based pushbroom-type images," *IEEE Transactions on Geoscience and Remote Sensing*, vol. 48, no. 4, pp. 1860–1871, 2010.

[8] Y. Chen, T. Z. Huang, and X. L. Zhao, "Destriping of multispectral remote sensing image using low-rank tensor decomposition," *IEEE Journal of Selected Topics in Applied Earth Observations and Remote Sensing*, vol. 11, no. 12, pp. 4950–4967, 2019.

[9] Y. Hu, D. Zhang, J. Ye, X. Li, and X. He, "Fast and accurate matrix completion via truncated nuclear norm regularization," *IEEE Transactions on Pattern Analysis and Machine Intelligence*, vol. 35, no. 9, pp. 2117–2130, 2013.

[10] J. M. Bioucas-Dias and M. A. T. Figueiredo, "A new twist: two-step iterative shrinkage/thresholding algorithms for image restoration," *IEEE Transactions on Image Processing*, vol. 16, no. 12, pp. 2992–3004, 2007.